

# A MODEL OF INTERPLANETARY AND CORONAL MAGNETIC FIELDS

KENNETH H. SCHATTEN and JOHN M. WILCOX

*Space Sciences Laboratory, University of California, Berkeley, Calif., U.S.A.*

and

NORMAN F. NESS

*Goddard Space Flight Center, Greenbelt, Md., U.S.A.*

(Received 22 July, 1968)

**Abstract.** A model of the large-scale magnetic field structure above the photosphere uses a Green's function solution to Maxwell's equations. Sources for the magnetic field are related to the observed photospheric field and to the field computed at a 'source' surface about  $0.6 R_{\odot}$  above the photosphere. The large-scale interplanetary magnetic field sector pattern is related to the field pattern at this 'source' surface. The model generates magnetic field patterns on the 'source' surface that compare well with interplanetary observations. Comparisons are shown with observations of the interplanetary magnetic field obtained by the IMP-3 satellite.

## 1. Introduction

Evidence for the interplanetary magnetic field being of solar origin was obtained by NESS and WILCOX (1964). They showed that the direction of the interplanetary magnetic field had a 27-day periodicity and that it correlated well with the average direction of the photospheric magnetic field during 3 solar rotations near the minimum of the last sunspot cycle. A  $4\frac{1}{2}$ -day time lag was found for the highest correlations, representing the time necessary for a radially flowing solar wind to transport the solar magnetic field to a position near the earth. Although high correlations were found for many latitudes, the recurrence period of the interplanetary magnetic field suggested a source on the photosphere  $10^{\circ}$  to  $15^{\circ}$  from the equator. Large-scale properties of the interplanetary magnetic field were also noted. It has been found that the interplanetary magnetic field as observed near the earth has a tendency to point predominantly 'away' from the sun or 'toward' the sun for a duration of several days. This pattern has been called the sector structure. The sector structure has been useful in ordering many interplanetary phenomena related to the solar wind (WILCOX and NESS, 1965; WILCOX, 1968). Although the interplanetary magnetic field is well ordered on a large scale, the photospheric magnetic field has the appearance of being structured on a smaller scale. This has led DAVIS (1965) to suggest that the interplanetary sectors originated from small regions on the sun, essentially 'nozzles', in which the field direction was essentially unidirectional. A contrary opinion has been supported by WILCOX (1968) where a 'mapping' hypothesis allows the sectors to originate from large, well-ordered magnetic structures on the sun in which there is a tendency for each longitude near the sun to be connected to a longitude at the orbit of the earth by magnetic field lines. By obtaining information related to the magnetic field patterns in

the inner corona, the origin of the sector patterns in the interplanetary medium can be further investigated.

A means of calculating the magnetic field structure on a small scale above the photosphere, utilizing a potential solution, was employed by RUST (1966). He showed that prominence magnetic fields had configurations similar to those obtained by potential theory, and that the material in prominences could be supported by the depressions situated at the tops of some field loops.

It was suggested by NEWKIRK (1967) that the potential dipole model appears capable of yielding a crude representation of the magnetic field above active regions and the more quiet portions of the sun. It was also stated that below about  $3 R_{\odot}$  the coronal material is controlled by the magnetic field. Support for this may be obtained from the observations of BUGOSLAVSKAYA (1949) from 1887 to 1945, that the highest closed arches in the eclipse data have a mean height of  $0.6 R_{\odot}$  above the limb. In addition, the maximum height of U bursts yields the same value and provides information that the magnetic field has roughly a 1 gauss value at this height (TAKAKURA, 1966).

## 2. Source Surface Model

A physical model that is consistent with many of the properties observed in the corona and in interplanetary space has been developed. The model is an attempt to account for the important effects that the magnetic field has upon the inner corona. A representation of the model is shown in Figure 1. There are three distinct regions in the model where different physical phenomena occur. Region 1 represents the photosphere, where the magnetic field motion is governed by the detailed motions of the plasma near the photosphere. Above the photosphere the plasma density diminishes very rapidly with only moderate decreases in the magnetic energy density. This results in region 2, where the magnetic energy density is greater than the plasma energy density and hence controls the configuration. We may then utilize the force-free condition,  $\mathbf{j} \times \mathbf{B} = 0$ , and in fact make the more restrictive assumption that region 2 is current free. The magnetic field in region 2 may then be derived from a potential that obeys the Laplace equation:  $\nabla^2 \phi = 0$ . The scalar potential may then be employed in the solution of the magnetic field configuration in this region. Using the less restrictive force-free condition would allow a 'twisting' of field lines or filamentary structure without substantially changing the large-scale magnetic structure.

Substantially further out in the corona the total magnetic energy density diminishes to a value less than the plasma energy density, and the magnetic field can then no longer structure the solar wind flow. The magnetic field has, however, become oriented very much in the radial direction, as suggested by DAVIS (1965). Thus, before the total magnetic energy density falls below the plasma energy density, a region is reached where the transverse magnetic energy density does so. It is the transverse magnetic field that interacts with the coronal plasma, since a radial magnetic field would neither affect nor be affected by a radially flowing plasma. Regions 2 and 3 are separated by the surface where the transverse magnetic energy density falls below the plasma energy

density. In region 3 transverse magnetic fields are transported by the radially flowing plasma, and can not exist in a quasi-static fashion. The magnetic field existing on the surface boundary between regions 2 and 3 is thus oriented in approximately the radial direction, and serves as a source for the interplanetary magnetic field. This 'source' surface is the region where currents in the corona cancel the transverse magnetic field. The region may not in fact be a surface but be a few tenths of a solar radius

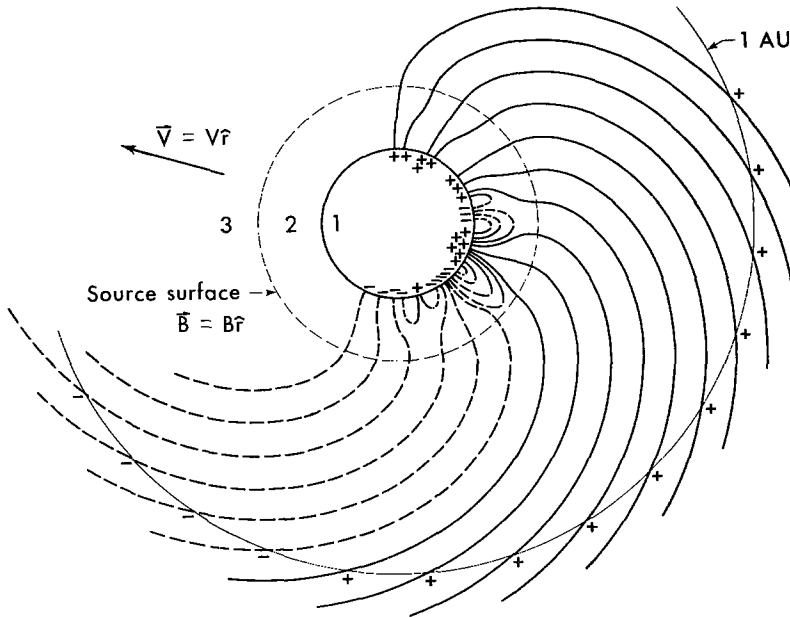


Fig. 1. Schematic representation of the source surface model. The photospheric magnetic field is measured in region 1 at Mount Wilson Observatory. Closed field lines (loops) exist in region 2. The field in this region is calculated from potential theory. Currents flowing near the source surface eliminate the transverse components of the magnetic field, and the solar wind extends the source surface magnetic field into interplanetary space. The magnetic field is then observed by spacecraft near 1 AU.

thick. Figure 2 illustrates the energy densities of various components of the solar atmosphere as a function of distance above the photosphere. The data for the figure were obtained by choosing moderate values for the densities, velocities, temperatures and magnetic field strengths within the solar cycle. The transverse magnetic energy density curve is obtained by utilizing the frozen field approximation and thus relating the ratio of the transverse field divided by the longitudinal field to the quantity  $nr^3$  (DAVIS, 1965). The energy curves shown are to be interpreted from a somewhat qualitative viewpoint in that uncertainties are likely to be near a factor of 10, and the representation of complex coronal structures by average values is somewhat misleading. The domination by the magnetic field in the inner corona can be seen. Above about  $0.7 R_{\odot}$  the transverse magnetic energy density falls below the plasma

energy density so that any closed field line configurations are transported out by the solar wind. Angular momentum is transferred to the solar wind by the magnetic field in this region. Near  $20 R_{\odot}$  the solar wind completely dominates the flow. WEBER and DAVIS (1967) give a description of this region.

A solution for the magnetic field inside the source surface is now obtained to permit comparisons of the model with observations. The source surface is approxi-

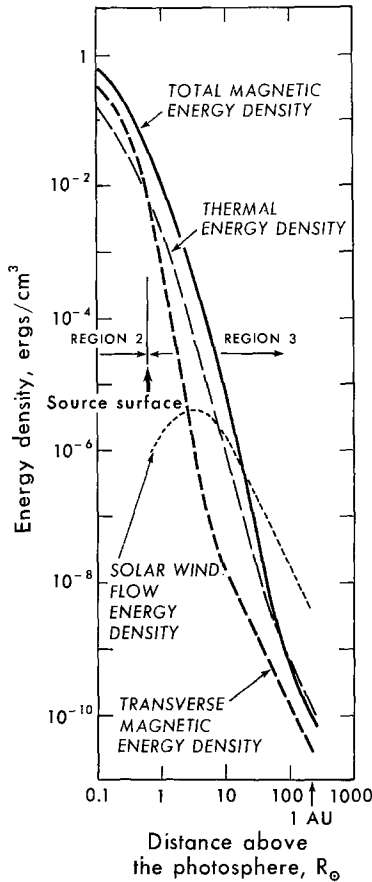


Fig. 2. The energy density of the total magnetic field, transverse magnetic field, thermal motions, and solar wind flow versus distance above the photosphere. In region 2 the magnetic field dominates coronal structures. On the source surface transverse magnetic fields are transported by the plasma, although the longitudinal magnetic field still transfers angular momentum to the solar wind. Beyond about  $20 R_{\odot}$  the solar wind dominates the flow motion.

mated as a concentric sphere with the radius  $R_S$ . A Green's function solution as shown in Figure 3 is then employed. A source of field lines on the sun is represented in a mathematical sense by a monopole of twice the field strength  $M$ . This factor of 2 is needed because half of the field lines from this source run into the sun and hence are

not seen. Utilization of a scalar potential  $\phi$  of the form shown in Figure 3 allows the magnetic field to obey the boundary conditions of a radially oriented field on the source surface. The magnetic field at any location above the photosphere and within the source surface is given by  $\mathbf{B}(\mathbf{R}_x) = -\nabla\phi$ . In particular, the magnetic field evaluated on the source surface is shown. The currents flowing on the source surface are given by  $\mathbf{J} = (c/4\pi)\nabla \times \mathbf{B}$ . The magnetic field due to the distribution of sources needed to represent actual observations is then calculated for a particular radius  $R_s$ . The magnetic fields calculated on the source surface can then be compared with interplanetary observations to determine  $R_s$  and to provide a test of the model. There will certainly be differences between the magnetic field on the source surface and the interplanetary field. The regularity of the interplanetary field, however, suggests that much of the ordering of the field near the sun has not been removed during this transport.

GREEN'S FUNCTION SOLUTION OF MAGNETIC FIELD INSIDE SOURCE SURFACE

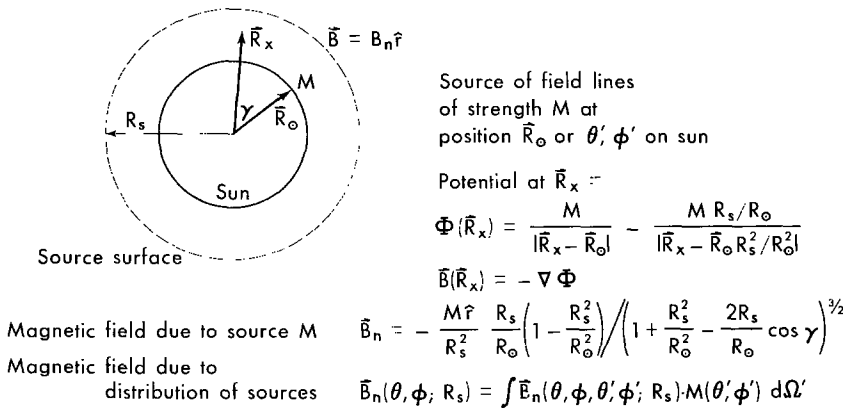


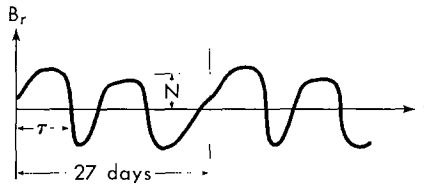
Fig. 3. The potential solution for the magnetic field produced by a source of field lines with a normal magnetic field boundary condition is shown. The magnetic field on the source surface  $\mathbf{B}_n$  is also calculated.

To calculate the magnetic field on the source surface, observations of the photospheric magnetic field obtained by the Mount Wilson Observatory for 9 solar rotations during the latter half of 1965 were utilized. An estimate for the solar magnetic field values of 7.0 gauss directed into the sun at latitudes Northward of  $65^\circ$  and 3.5 gauss directed away from the sun Southward of  $65^\circ$  in the Southern hemisphere was employed (HOWARD, private communication). Observationally, the magnetic field over a solar rotation does not average to zero. To preserve the divergence free requirement of the magnetic field, a uniform field over the entire sun was added to the observations for each solar rotation. This additional field was, with one exception, less than a gauss. This is small compared to the quantization level of the photospheric measurements.

### 3. Results and Discussion

The behavior of the solution is illustrated in Figure 1. In region 2 closed magnetic loops form above photospheric regions of opposite polarity. These magnetic configurations have the appearance of the helmet streamers seen in coronal photographs. The parametric dependence of the magnetic field on the source surface upon  $R_S$  is such that for values of  $R_S$  not much greater than  $R_\odot$ , the magnetic field on the source surface appears very much like the photospheric field. As  $R_S$  is increased, the presence of magnetic loops above the photosphere results in fewer magnetic field lines reaching the source sphere. Small-scale magnetic field structures on the photosphere tend to produce small-scale loops, and do not make their presence known on the source surface. The source surface tends to smooth out the photospheric field on a scale comparable to  $R_S - R_\odot$ . Thus the solution tends to explain qualitatively the reasons for the interplanetary field being unidirectional for several days while the photospheric field is more filamentary. We can use these ideas in a quantitative manner to find the best value for the parameter  $R_S$ .

CHARACTERISTICS OF PERIODIC FUNCTION RELATED TO PHOTOSPHERIC-INTERPLANETARY MAGNETIC FIELD STUDIES



1. Average amplitude  $\rightarrow$  Number of field lines =  $N$
2. Characteristic frequency  $\rightarrow$  Duration of unidirected region =  $\tau$



3. Shape of function  $\rightarrow$  RMS deviation of unidirected region

Fig. 4. This figure illustrates three characteristics that can be used to qualitatively describe the nature of the magnetic field between the photosphere and interplanetary space. These three characteristics are plotted in the following three figures as a function of distance above the photosphere.

The magnetic field pattern near the earth, on the sun, and on the source sphere is roughly a periodic function with a 27-day period. As Figure 4 illustrates, this pattern can be characterized by the number of magnetic field lines, the average duration of a unidirectional region, and the RMS deviation of unidirectional regions (a measure of the shape of the pattern). These quantities were calculated from the magnetic fields on source surfaces at distances ranging from  $0.25 R_\odot$  to  $1.0 R_\odot$  above the photosphere. Figure 5 shows the average number of magnetic field lines per unit solid angle reaching the source surface as a function of distance above the photosphere,  $(R_S - R_\odot)$ , on a

semilog scale. On the ordinate axis are plotted the values corresponding to the Mount Wilson Observatory photospheric observations at various latitudes ranging from  $30^{\circ}\text{S}$  to  $30^{\circ}\text{N}$ . Above the photosphere the values are calculated utilizing the source surface model. As expected, as  $R_s$  increases the number of field lines reaching the surface decreases. The average observed interplanetary field is represented by the dashed line whose value is independent of distance from the sun, since the radial component of the field in the solar wind varies as  $1/R^2$  and therefore has a constant number of field lines per unit solid angle. It is interesting that the  $0^{\circ}$ -curve has a low ordinate value but decreases less sharply than the other latitude curves. This is related to the low magnetic activity near the equator. As  $R_s$  increases, however, higher

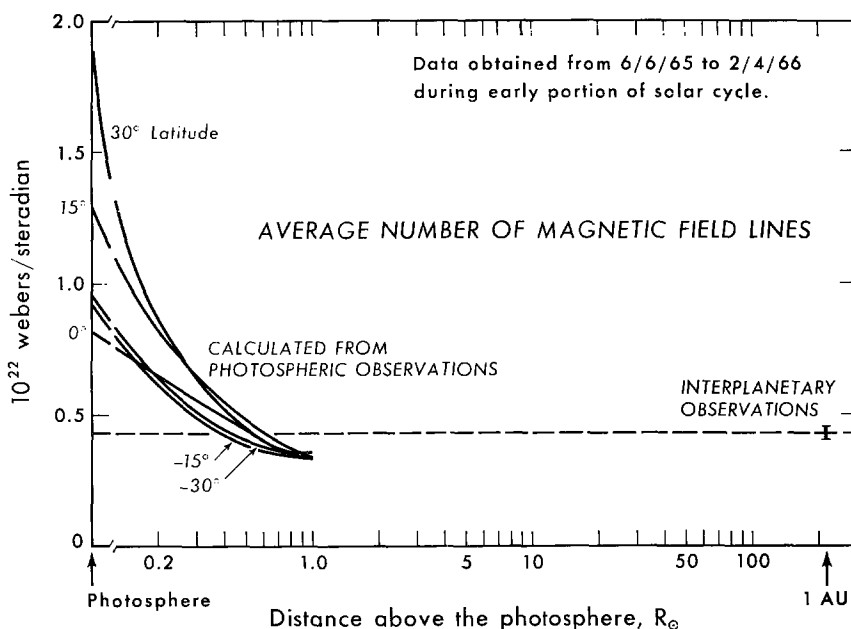


Fig. 5. Average number of magnetic field lines as a function of distance above the photosphere. The average values for the photospheric observations are plotted on the ordinate axis for latitudes ranging from  $30^{\circ}\text{S}$  to  $30^{\circ}\text{N}$ . Magnetic fields calculated on source surfaces are used to determine values between  $0.25$  and  $1.0 R_{\odot}$  above the photosphere. Agreement with interplanetary observations occurs on a source surface near  $0.6 R_{\odot}$  above the photosphere.

latitude activity has an increasing influence on the  $0^{\circ}$ -curve, resulting in a more gradual decline. Utilizing the crossover point between interplanetary observations and calculations from the source surface model, we obtain a value of  $R_s$  of  $0.4 R_{\odot}$ – $0.7 R_{\odot}$  above the photosphere. It is interesting that at this radius roughly one third of the photospheric magnetic field lines reach the source surface.

Figure 6, produced in the same format, is a plot of the average duration of a unidirected region. There is an increase in the duration of these regions as  $R_s$  increases. A comparison with the average duration of an interplanetary sector fixes  $R_s$  at

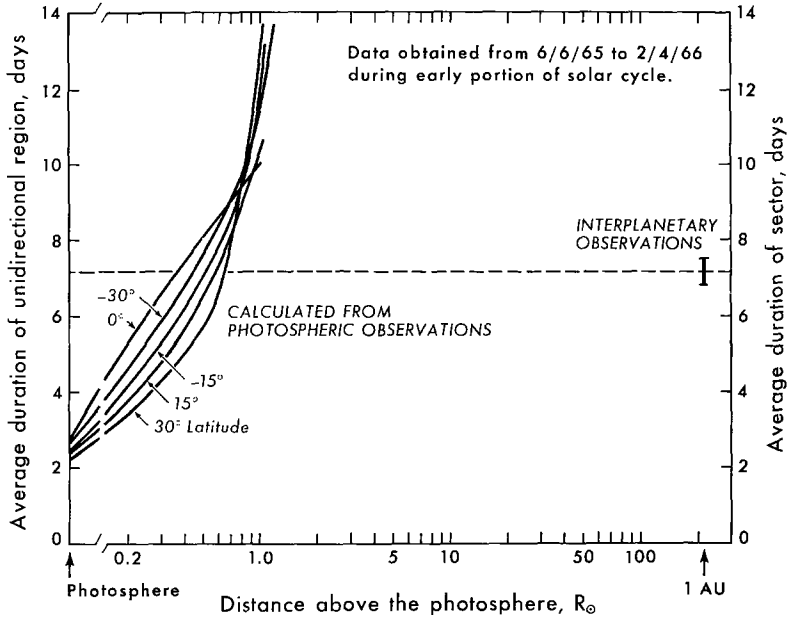


Fig. 6. Average duration of unidirectional regions as a function of distance above the photosphere plotted for 5 ranges of latitudes. Agreement with interplanetary observations occurs on a source surface between 0.4 and 0.7  $R_{\odot}$  above the photosphere.

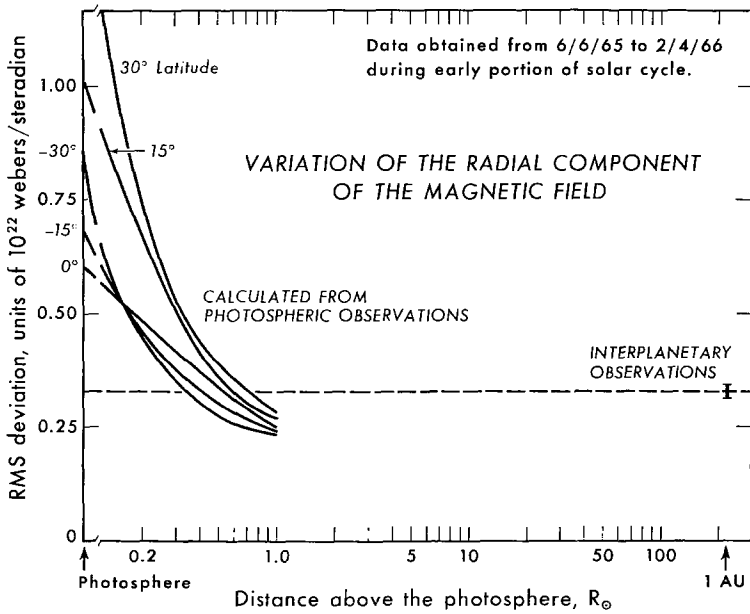


Fig. 7. Variation of the radial component of the magnetic field determined by using the RMS deviation of unidirectional regions as a function of distance above the photosphere. Agreement with interplanetary observations occurs between 0.4 and 0.8  $R_{\odot}$  above the photosphere.



approximately the same value, perhaps about  $0.5 R_{\odot}$  above the photosphere. This figure clarifies the origin of sectors. As  $R_s$  increases, an increasing number of lines of force in the filamentary photospheric field pattern loop back to the photosphere. At  $0.6 R_{\odot}$  the remaining field pattern is frozen into the solar wind and carried outward. If  $R_s$  were to decrease, the sector pattern would be more filamentary in nature.

The variation of the radial component of the magnetic field is shown in Figure 7, plotted in the same manner. Agreement also occurs between  $0.4 R_{\odot}$  to  $0.8 R_{\odot}$  above the photosphere. Thus three properties of the interplanetary magnetic field can be reconstructed from this model: the average field strength, the average sector duration and the field variation throughout a sector.

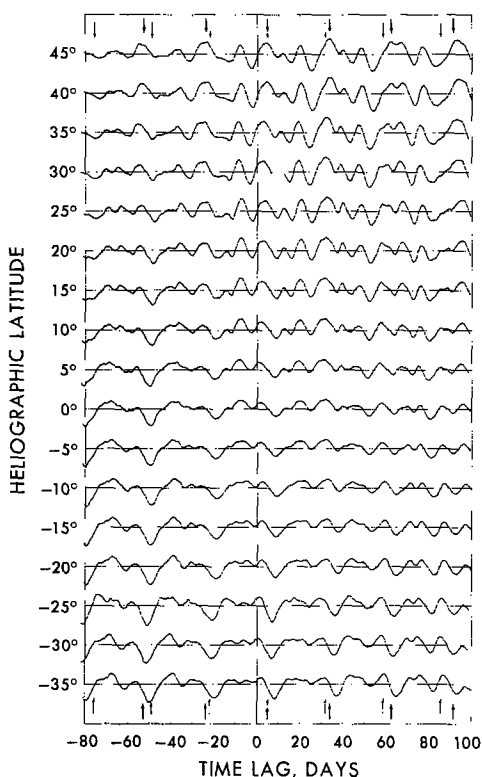


Fig. 8. Cross-correlation of the magnetic field calculated on a source surface  $0.5 R_{\odot}$  above the photosphere with the radial component of the interplanetary magnetic field as a function of time lag. Nine solar rotations of data are utilized, with correlations extending from  $35^{\circ}\text{S}$  to  $45^{\circ}\text{N}$  in intervals of  $5^{\circ}$ . Arrows at the bottom of the graph indicate time lags of 5 days plus an integral number of solar rotations.

As a check of the model a direct correlation with interplanetary data is shown in Figure 8. This figure shows a cross-correlation of the magnetic field calculated at  $0.5 R_{\odot}$  above the photosphere and the radial component of the interplanetary field observed during nine solar rotations. Correlations for latitudes ranging from  $\text{N } 45^{\circ}$

to S  $35^\circ$  are shown. The scale of the ordinate for each graph is such that  $+1.0$  lies on the line above each graph and  $-1.0$  lies on the line beneath. The abscissa is time lag in days. Correlations are obtained at intervals of 12 hours. The small arrows at the bottom and top of the graph indicate time lags of 5 days plus integral numbers of 27-day intervals. The larger arrows indicate time lags of 5 days plus integral numbers of 29-day intervals. Peaks are seen near the 5-day time lag for various latitudes corresponding to those observed by NESS and WILCOX (1964). A larger correlation is observed near a lag of 33 days. This indicates that new magnetic fields reaching the photosphere require roughly one solar rotation before their effects become present in the interplanetary medium. Peaks near 60 days and 80 days, comparable to the 5-day

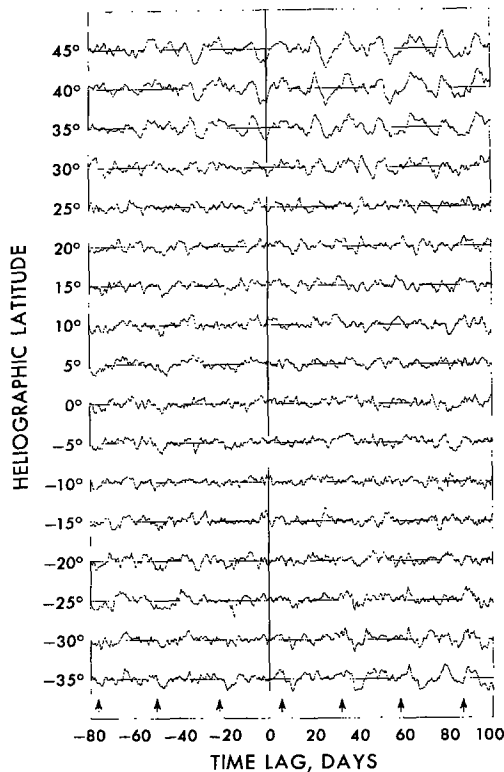


Fig. 9. Same as Figure 8, except that the magnetic field calculated on the source surface is replaced by the field observed in the photosphere. Note the lack of correlation.

peak, are also observed. The spacing between the peaks indicates a periodicity of the field larger than 28 days. This suggests that the photospheric source of the interplanetary plasma and field observed near the earth at this time may be poleward of  $25^\circ$ . One can think of the 5-day peak as a measure of the quasi-static magnetic features on the photosphere. The fact that the 33-day peaks are larger than the 5-day peaks indicates a more rapid evolution of magnetic fields than existed during the time near

solar minimum observed by IMP-1.\* A particular example illustrating the delay of about one solar rotation for the evolution of a new photospheric magnetic feature into interplanetary space was observed by SCHATTEN *et al.* (1968).

Figure 9, prepared in the same manner as Figure 8, shows a cross-correlation of the observed photospheric magnetic fields with interplanetary field observations. The appearance of the figure is one of random fluctuations with no coherent correlation existing. The effect of the source surface model is to remove the small scale fluctuating features existing in the photospheric pattern that do not make their presence known in the interplanetary medium, and thus organizes the pattern to a form more similar to the sector structure, as shown in Figure 8.

Figure 10 is a synoptic chart of the photospheric magnetic field obtained by the Mount Wilson Observatory for Carrington solar rotation 1496. The dark gray regions represent magnetic field into the sun and the light gray regions represent magnetic

Fig. 10. A synoptic chart of the photospheric magnetic field obtained by the Mount Wilson Observatory for Carrington solar rotation 1496. The dark gray regions represent magnetic field into the sun, the light gray regions magnetic field out of the sun. The contour levels are 6, 12, 20 and 30 gauss. Contours of the magnetic field on a source surface  $0.5 R_{\odot}$  above the photosphere are shown. Dashed contours represent field directed towards the sun and solid contours field directed away from the sun. Dotted contours represent regions of zero field. Contour levels are 0.25 and 0.75 gauss. Also shown at the bottom of the figure are the interplanetary sector structure and magnetic field magnitude displaced by 5 days. Toward sectors are represented by heavy shading, away sectors by light shading, and mixed polarity fields by diagonal shading.

\* This may be understood as follows. If there were no evolution of solar magnetic features then the 5-day peak, the 33-day peak and the subsequent peaks would be of equal amplitude. New photospheric magnetic features do appear, however, and these features do evolve with time. The appearance of a new photospheric magnetic feature does enter into the Green's function calculation and from the smaller cross-correlation at 5 days than at 33 days, it does not have an immediate effect on the interplanetary magnetic field. Its influence on the interplanetary magnetic sector structure is only apparent after a delay of about a solar rotation.

field out of the sun. The contours of the magnetic field calculated on a source surface  $0.5 R_{\odot}$  above the photosphere are shown superimposed. The solid contours represent magnetic field directed away from the sun, the dashed contours represent field toward the sun and the dotted contours represent the boundaries between regions of oppositely-directed fields. At the bottom of the figure is a strip representing the sector pattern of the interplanetary magnetic field displaced by 5 days, and a graph of the interplanetary field magnitude. Toward-the-sun sectors are represented by heavy shading and away-from-the-sun sectors by light shading. A region of mixed polarity is represented by diagonal shading.

The smoothing of the photospheric field to a more sector-like pattern on the source surface is evident. In the regions of the source surface where the field magnitude has reached the first contour level the agreement with the direction of the interplanetary field is very good. The low magnitude of the interplanetary magnetic field from July 10 through July 14 may be related to the low field magnitude on the source surface at these times. On either side of this interval both the interplanetary field and the source surface fields have larger magnitudes. The source surface model allows a direct comparison of field magnitudes in interplanetary space with those predicted from photospheric observations, whereas previous analyses included only directional comparisons.

The magnetic field contours on the source surface in Figure 10 appear to be centered on features at fairly high latitudes, perhaps  $30^{\circ}\text{N}$ – $35^{\circ}\text{N}$ . This suggests that low latitude regions on the source surface tend to be connected by magnetic field lines to fairly high latitude regions on the photosphere.

The away-from-the-sun sector on July 18 through July 22 is also closely associated with the pattern on the source surface. The photospheric magnetic field exhibits in the Northerly latitudes a large unidirected region near July 19 that has sufficient flux to account for both the source surface magnetic flux seen throughout this sector and the interplanetary flux. The photospheric background field is of mixed polarity with perhaps a dominance of toward-the-sun magnetic features. This suggests that the magnetic feature near July 19 at  $30^{\circ}\text{N}$  may be responsible for the away-from-the-sun sector at this time. This suggests rather than a one-to-one mapping of photospheric to interplanetary magnetic features a certain amount of non-radial expansion is occurring during this sector. The amount of non-radial expansion during this sector may be close to 1:3. This may represent a viewpoint intermediate between the 'mapping' hypothesis and the 'nozzle' hypothesis in that a certain amount of non-radial expansion is occurring but not a very large amount. The exact amount of non-radial expansion occurring may be better understood by mapping out the magnetic field lines between the photosphere and the source surface. It is also important to note that the amount of non-radial expansion may change from sector to sector and may vary during the course of the 11-year solar cycle.

The persistent solar magnetic pattern discussed by WILCOX and HOWARD (1968) has the property that over a range of heliographic latitudes from at least  $40^{\circ}\text{N}$  to  $35^{\circ}\text{S}$  the stretching to be expected from differential rotation is almost absent. In

Figure 8 the peaks near 5 days and near 33 days in the cross-correlations between the interplanetary field and the source surface field are at time lags that vary only a small amount with latitude. Since the peaks near 33 days are the largest they have been selected for further analysis. Figure 11 shows the position (lag) of each of these peaks as a function of heliographic latitude. The almost-constant position of these peaks is consistent with the persistent solar magnetic pattern discussed by WILCOX and HOWARD (1968). (See their Figure 3 and associated text for a further discussion of this point.)

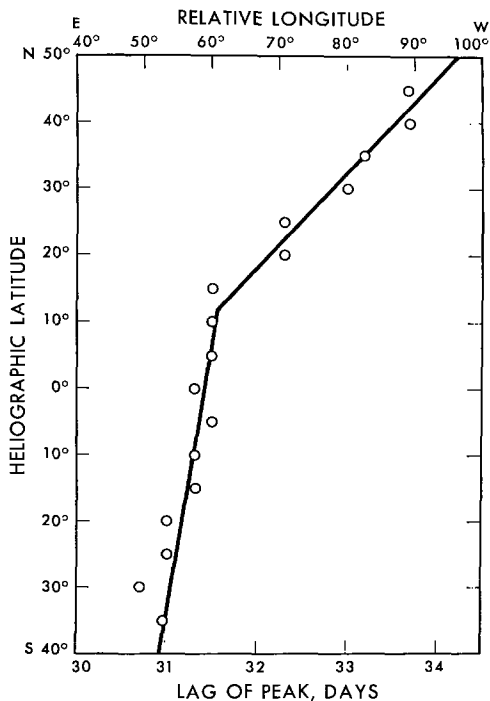


Fig. 11. Position of the peaks near 33 days in Figure 8 as a function of heliographic latitude. The relative longitude scale is explained in WILCOX and HOWARD (1968), Figure 3. The two straight lines are drawn by eye.

During 1964 (near solar minimum) the correlations between solar and interplanetary fields had approximately the same large-scale shape at all heliographic latitudes examined, suggesting that the persistent solar pattern was approximately the same at all these latitudes. In the interval from June 1965 to February 1966 shown in Figure 8 the shape of the correlations in the Northern solar hemisphere is somewhat different from that in the Southern hemisphere, suggesting that the persistent solar magnetic pattern may be different in some details from North to South.

Since the cross-correlations in the final quarter of 1964 had become very small (WILCOX and HOWARD, 1968), it is of interest that in 1965 they are again quite prominent. Of course, the source surface analysis employed in the present paper is

different from the comparison of photospheric and interplanetary field directions used in the earlier work.

### Summary

A source surface model which allows the large-scale magnetic field structure above the photosphere to be computed from photospheric magnetic observations utilizes a Green's function solution to Maxwell's equations. The boundary conditions for the solution are the magnetic observations on the photosphere and a radially oriented field on a source surface about  $0.6 R_{\odot}$  above the photosphere. The position of the source surface is approximately determined by comparisons with the interplanetary field.

The magnetic field calculated on the source surface allows comparisons with interplanetary magnetic field magnitudes for the first time. The magnetic field calculated on the source surface agrees reasonably well both qualitatively and explicitly with interplanetary magnetic field observations.

It is suggested that new photospheric magnetic features do not make their presence known to the interplanetary medium for approximately a solar rotation. The photospheric source for the interplanetary field during this period appears to be poleward of  $25^{\circ}$ . The 'nozzle' and 'mapping' hypotheses are discussed with reference to this model.

### Acknowledgements

The authors are grateful to R. Howard for kindly providing Mount Wilson Observatory synoptic charts used in the analysis.

This research was supported in part by the Office of Naval Research under Contract Nonr 3656(26), by the National Aeronautics and Space Administration under Grants NsG 243 and NGR 05-003-230, and by the National Science Foundation under Grant GA 1319. One of us (KHS) would also like to acknowledge support from the National Science Foundation.

### References

- BUGOSLAVSKAYA, E. Y.: 1949, *Publ. Sternberg Inst.* No. 19.  
DAVIS, L.: 1965, in *Stellar and Solar Magnetic Fields* (ed. by R. Lüst), North-Holland Publ. Co., Amsterdam.  
NESS, N. F. and WILCOX, J. M.: 1964, *Phys. Rev. Letters* **13**, 461.  
NEWKIRK, G. A.: 1967, *Ann. Rev. Astron. Astrophys.*, Vol. 5, p. 213.  
RUST, D. M.: 1966, Thesis, University of Colorado, Boulder.  
SCHATIEN, K. H., NESS, N. F., and WILCOX, J. M.: 1968, *Solar Phys.* **5**, 240.  
TAKAKURA, T.: 1966, *Space Sci. Rev.* **5**, 80.  
WEBER, E. J. and DAVIS, L.: 1967, *Astrophys. J.* **148**, 217.  
WILCOX, J. M.: 1968, *Space Sci. Rev.* **8**, 258.  
WILCOX, J. M. and NESS, N. F.: 1965, *J. Geophys. Res.* **70**, 5793.  
WILCOX, J. M. and HOWARD, R.: 1968, *Solar Phys.* **5**, 564.